Citation: Cell Death and Disease (2012) 3, e346; doi:10.1038/cddis.2012.82

www.nature.com/cddis

Induction of robust *de novo* centrosome amplification, high-grade spindle multipolarity and metaphase catastrophe: a novel chemotherapeutic approach

V Pannu[1], PCG Rida[1], A Ogden[1], R Clewley[2], A Cheng[1], P Karna[1], M Lopus[3], RC Mishra[1], J Zhou[4] and R Aneja*[,1]

Centrosome amplification (CA) and resultant chromosomal instability have long been associated with tumorigenesis. However, exacerbation of CA and relentless centrosome declustering engender robust spindle multipolarity (SM) during mitosis and may induce cell death. Recently, we demonstrated that a noscapinoid member, reduced bromonoscapine, (S)-3-(R)-9-bromo-5-(4,5-dimethoxy-1,3-dihydroisobenzofuran-1-yl)-4-methoxy-6-methyl-5,6,7,8-tetrahydro-[1,3]dioxolo-[4,5-g]isoquinoline (Red-Br-nos), induces reactive oxygen species (ROS)-mediated autophagy and caspase-independent death in prostate cancer PC-3 cells. Herein, we show that Red-Br-nos induces ROS-dependent DNA damage that resulted in high-grade CA and SM in PC-3 cells. Unlike doxorubicin, which causes double-stranded DNA breaks and chronic G2 arrest accompanied by 'templated' CA, Red-Br-nos-mediated DNA damage elicits *de novo* CA during a transient S/G2 stall, followed by checkpoint abrogation and mitotic entry to form aberrant mitotic figures with supernumerary spindle poles. Attenuation of multipolar phenotype in the presence of tiron, a ROS inhibitor, indicated that ROS-mediated DNA damage was partly responsible for driving CA and SM. Although a few cells (~5%) yielded to aberrant cytokinesis following an 'anaphase catastrophe', most mitotically arrested cells (~70%) succumbed to 'metaphase catastrophe,' which was caspase-independent. This report is the first documentation of rapid *de novo* centrosome formation in the presence of parent centrosome by a noscapinoid family member, which triggers death-inducing SM via a unique mechanism that distinguishes it from other ROS-inducers, conventional DNA-damaging agents, as well as other microtubule-binding drugs.

Cell Death and Disease (2012) **3,** e346; doi:10.1038/cddis.2012.82; published online 12 July 2012
Subject Category: Cancer

Cancer cells are often characterized by centrosome amplification (CA) and chromosomal instability.[1] Although supernumerary centrosomes can be tumor-promoting by inducing low-grade aneuploidy, they present a potential for multipolar mitoses that may lead to high-grade, death-inducing aneuploidy.[2] To escape a multipolar configuration, cancer cells have evolved 'clever' tactics to suppress multipolarity by pseudo-bipolar centrosome clustering during mitosis.[3,4] Because cancer cells are inherently vulnerable to induction of CA unlike normal cells,[3,5] any CA-inducing agent is likely to carry the additional advantage of being cancer cell-specific. An emerging paradigm thus ascribes robust induction of spindle multipolarity (SM) by CA and persistent centrosome declustering as a potentially attractive two-pronged chemotherapeutic approach.[6,7] Thus, strategies exploiting powerful induction of supernumerary centrosomes are becoming center stage for cancer-selective therapeutic intervention.

Cell-cycle progression is intimately integrated with oscillations in oxygen consumption, energy metabolism and redox state, all of which rely on reactive oxygen species (ROS) levels.[8,9] Because the array of targets that respond to changes in redox status fluctuate during the cell cycle, ROS levels affect cell fate variably.[9] Centrosomes, also called 'command centers for cellular control', have been recently identified as an integration hub of several signaling pathways, including the DNA-damage response for cell-cycle arrest and repair following ROS-mediated stress.[10,11] Several reports suggest existence of a centrosome inactivation checkpoint that utilizes DNA-damage-induced CA to provoke cell death during mitosis, referred to as 'mitotic catastrophe'.[10] However, cells refractory to mitotic catastrophe may proceed to yield multiple karyotypically unstable or nonviable daughter cells. This has been recently named 'anaphase catastrophe,' a phenomenon that can be pharmacologically induced for selective targeting of cancer cells.[12]

Continued efforts in our laboratory are focused on expanding a novel class of microtubule (MT)-modulating anticancer agents, noscapinoids, based upon the founding molecule,

[1]Department of Biology, Georgia State University, Atlanta, GA, USA; [2]Department of Mathematics and Statistics, Neuroscience Institute, Georgia State University, Atlanta, GA, USA; [3]Department of Molecular, Cellular, and Developmental Biology and the Neuroscience Research Institute, University of California, Santa Barbara, CA, USA and [4]Department of Genetics and Cell Biology, College of Life Sciences, Nankai University, Tianjin, China
*Corresponding author: R Aneja, Department of Biology, Georgia State University, 100 Piedmont Avenue, Atlanta, GA 30303, USA. Tel: 404 413 5417; Fax: 404 413 5301; Email: raneja@gsu.edu
Keywords: microtubule dynamics; tubulin-binding agent; *de novo* centrosome amplification; centrosome declustering; metaphase catastrophe
Abbreviations: CA, centrosome amplification; SM, spindle multipolarity; ROS, reactive oxygen species; MT, microtubule; ATM, ataxia-telangiectasia-mutated; ATR, ATM- and Rad3-related; Red-Br-nos, reduced bromonoscapine, (S)-3-(R)-9-bromo-5-(4,5-dimethoxy-1,3-dihydroisobenzofuran-1-yl)-4-methoxy-6-methyl-5,6,7,8-tetrahydro-[1,3]dioxolo-[4,5-g]isoquinoline; PCM, pericentriolar material; PLK4, polo-like kinase-4; MPM-2, mitotic protein monoclonal-2; SAC, spindle-assembly checkpoint
Received 27.9.11; revised 24.5.12; accepted 24.5.12; Edited by A Stephanou

noscapine.[13–15] Unlike conventional tubulin-binding agents, these small molecules gently attenuate MT dynamics without altering the total polymer mass of tubulin.[6,16,17] A novel noscapinoid, reduced bromonoscapine, (S)-3-(R)-9-bromo-5-(4,5-dimethoxy-1,3-dihydroisobenzofuran-1-yl)-4-methoxy-6-methyl-5,6,7,8-tetrahydro-[1,3]dioxolo-[4,5-g]isoquinoline (hereon referred to as Red-Br-nos), is significantly more potent than noscapine and its extensively studied congener, 9-bromonoscapine (also known by EM011).[16,18,19] Recently, we reported that Red-Br-nos induces mitochondrially driven ROS-dependent autophagic cell death that was caspase-independent in prostate cancer PC-3 cells.[19] However, key cell-cycle events responsive to ROS induction that can intercede life and death decisions upon Red-Br-nos exposure still remain elusive. Herein, we take the study to the next level by closely investigating outcomes of Red-Br-nos-induced ROS production on cell-cycle phase-specific events and analyzing how that translates into cell death in a caspase-refractory setting in prostate cancer cells.

Our data demonstrate that Red-Br-nos induces ROS-dependent DNA damage, which causes *de novo* CA associated with increased cdk2 activity and enhanced polo-like kinase-4 (PLK4) expression. Despite activation of DNA-damage-sensitive kinases, cells were transiently arrested in S or G2 phases and bypassed the DNA-damage checkpoint to enter mitosis. Induction of CA during interphase preceded generation of SM during a stalled mitosis, which was responsive to ROS-mediated DNA damage. This is the first report to identify induction of CA and consequent SM, which promotes mitotic death, in particular 'metaphase catastrophe', as the *modus operandi* for a member of the MT-modulating noscapine family.

Results

Red-Br-nos-induced ROS-dependent genotoxic stress activates a DNA-damage checkpoint response. Several studies suggest that ROS may directly modulate cell-cycle progression.[8] Depending upon the magnitude and duration of ROS exposure, activation of growth-factor-stimulated signaling cascades may promote cell-cycle progression upon low levels of ROS exposure or cause growth arrest upon prolonged ROS exposure.[8] Oxidative damage produced by intracellular ROS often results in DNA-based modifications and single- and double-strand breaks. This may alert a 'salvage' strategy like checkpoint surveillance to stall the cell cycle or a 'disposal' mechanism like apoptosis to eliminate irreparable cells.[20] We have recently demonstrated that Red-Br-nos (25 μM) causes ROS induction in PC-3 cells[19] as well as at a lower dose of 10 μM (Supplementary Figure 6B). Thus, we first asked whether Red-Br-nos-induced ROS causes DNA damage in PC-3 cells. To this end, we microscopically examined drug-treated cells over time for the presence of foci of γ-H2AX, the phosphorylated form of histone H2AX that forms around sites of DNA breakage.[20] Phosphorylation of H2AX (γ-H2AX) is an early chromatin modification and a sensitive marker for double-strand breaks.[20] We observed γ-H2AX foci as early as 3 h post Red-Br-nos treatment and a peak at 18 h, demonstrating a time-dependent increase in DNA damage throughout interphase (Figure 1ai). On the contrary, vehicle-treated control cells lacked γ-H2AX foci, indicating that drug exposure induced DNA-strand breaks. There was not only a time-dependent increase in number of cells with γ-H2AX foci but also an increase in the number and intensity of γ-H2AX foci per cell, indicating a rise in the extent and severity of DNA damage inflicted by Red-Br-nos over time (Figures 1aii and iii).

We next asked if γ-H2AX foci recruit additional proteins involved in the DNA-damage checkpoint response. The serine/threonine protein kinases ataxia-telangiectasia-mutated (ATM) and ATM- and Rad3-related (ATR) are transducers of DNA-damage checkpoint responses.[21] Although ATM responds to IR-induced double-strand breaks and activates chk2, ATR responds to DNA-damaging agents such as UV light and activates chk1.[22] Activated chk2 and chk1 in turn inactivate cdc25C phosphatase by phosphorylation, which leads to a G2/M arrest.[22] Although ATM levels remained unaffected by Red-Br-nos (data not shown), we found enhanced p-ATR expression, which perhaps increased chk1 activation, constituting a DNA-damage checkpoint response to Red-Br-nos treatment (Figure 1b).

Having identified Red-Br-nos-induced DNA-strand breaks, we next addressed whether induction of DNA damage was ROS-dependent. To this end, PC-3 cells were pretreated for 4 h with tiron, a ROS scavenger, and γ-H2AX foci were examined after 12 h of Red-Br-nos exposure (Figure 1ci). Attenuation of ROS levels by tiron decreased the number of cells with γ-H2AX foci by $\sim$88% following 12 h Red-Br-nos treatment (Figure 1ci, Supplementary Figure 1). This contrasted with Red-Br-nos treatment alone that caused an induction ($\sim$90%) of γ-H2AX foci-containing cells (Supplementary Figure 1). Attenuation of Red-Br-nos induced γ-H2AX levels upon tiron treatment was also confirmed by immunoblotting (Figure 1cii). However, we also saw low levels of γ-H2AX expression upon tiron treatment alone. Although several studies including ours have shown that tiron acts as a ROS scavenger,[19,23] there are reports that high-concentration tiron ($>$0.5 mM) induces ROS-independent DNA damage.[24] In our study, we used tiron at 1 mM, and this concentration likely resulted in low-level ROS-independent DNA damage.

Red-Br-nos-induced DNA damage mediates high-grade CA. Consonant with its protective function, the DNA-damage response may serve as an anticancer barrier in early human tumorigenesis.[25] One important mediator of the DNA-damage response, chk1, negatively regulates G2/M transition via its centrosomal localization, emphasizing a role for centrosomes in the DNA-damage response.[26] Centrosomes may serve as spatiotemporal organizers that juxtapose DNA checkpoint players in a defined manner.[10] Alternatively, if the centrosome cycle is regulated by DNA damage, centrosomes might serve as effectors of DNA-damage response, resulting in apoptosis-inducing centrosome inactivation or fragmentation.[10,27] Yet, another possibility is that activation of the DNA-damage response might trigger CA. To investigate effects of drug-induced DNA damage on centrosomes, we immunostained PC-3 cells with γ-tubulin, a centrosome-specific marker. We observed several γ-tubulin spots ranging from 2 to 11 per cell as early

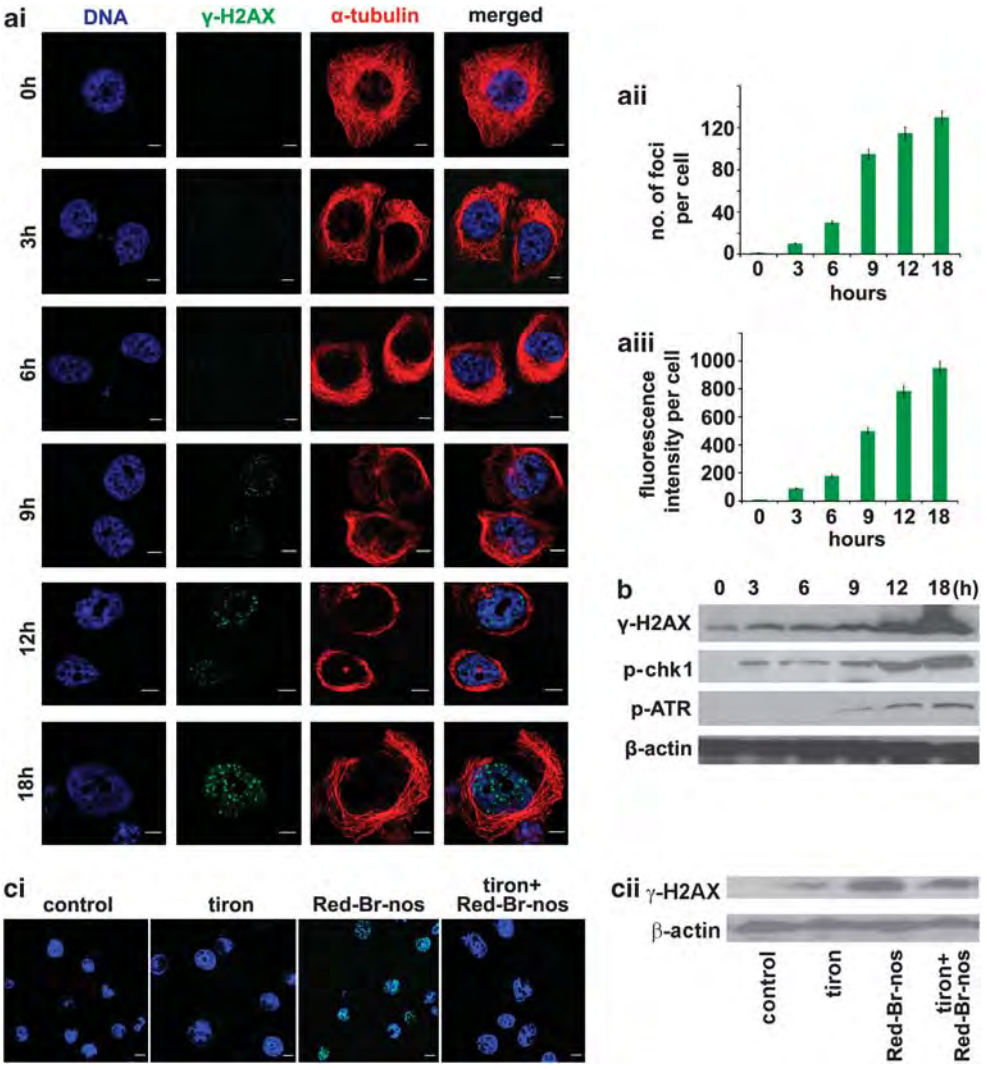

Figure 1 Red-Br-nos triggers ROS-mediated DNA-damage checkpoint response in PC-3 cells. (**ai**) Representative immunofluorescence confocal micrographs showing emergence of γ-H2AX foci indicative of DNA damage upon treatment with Red-Br-nos (10 μM) over time. Panels show DNA (DAPI), γ-H2AX (green) and MTs (red). (**aii** and **iii**) Bar-graph quantitation of number and intensity, respectively, of γ-H2AX foci per cell over time. (**b**) Immunoblot analysis of γ-H2AX and DNA-damage checkpoint response markers, p-ATR and p-chk1, at the noted time points. β-actin was used as the loading control. (**ci**) Attenuation of ROS upon a 4-h tiron treatment prior to Red-Br-nos exposure for 12 h showed a marked reduction in the number of cells harboring γ-H2AX foci (green) as compared with drug treatment alone. (**cii**) Immunoblot showing significant reduction in γ-H2AX expression when tiron was co-treated with drug compared with drug alone. Scale bar = 5 μm

as 12 h post drug treatment (Figures 2ai and ii). Intriguingly, we observed that ~70% of drug-treated cells showed an abnormal number of centrosomes ($n>2$). Although γ-tubulin is a centrosomal protein, its pericentriolar material (PCM) distribution is well known. Thus, to rule out centrosome fragmentation, we immunostained Red-Br-nos-treated cells with centrin-2, a specific centriolar marker (Figures 2bi and ii). Immunofluorescence confocal micrographs revealed several centrin spots in cells treated with Red-Br-nos for 12 h, suggesting that drug-treated cells exhibit 'true' CA involving generation of 'real' centrioles rather than just PCM fragmentation. These findings were further supported by our observations of time-lapse imaged, live MDA-MB-231 cells stably transfected with GFP-centrin that were treated with 10 μM Red-Br-nos for 9 h. We found that drug treatment induced extensive centriole amplification within 3 h (Supplementary Movie 1) unlike vehicle-treated control MDA-MB-231 cells (Supplementary Movie 2).

Several mitotic kinases, including PLK4 and Aurora A, have been shown to regulate centrosome-duplication events.[28,29] Importantly, PLK4 is not only implicated in centriole over-duplication[30] but also has been shown to deposit centriole precursor material in a rosette-like arrangement around maternal centrioles.[31] Thus, we wanted to determine whether Red-Br-nos-induced CA was accompanied by enhanced PLK4 expression levels in PC-3 cells. Immunofluorescence as well as immunoblotting data confirmed the increase in PLK4 expression upon drug treatment (Figures 2c and d). Interestingly, drug treatment increased cdk2 activity, as seen by enhanced expression of phosphohistone-H3 (Figure 2e). Pretreatment with tiron before drug exposure attenuated the number of cells harboring multiple centrosomes, suggesting

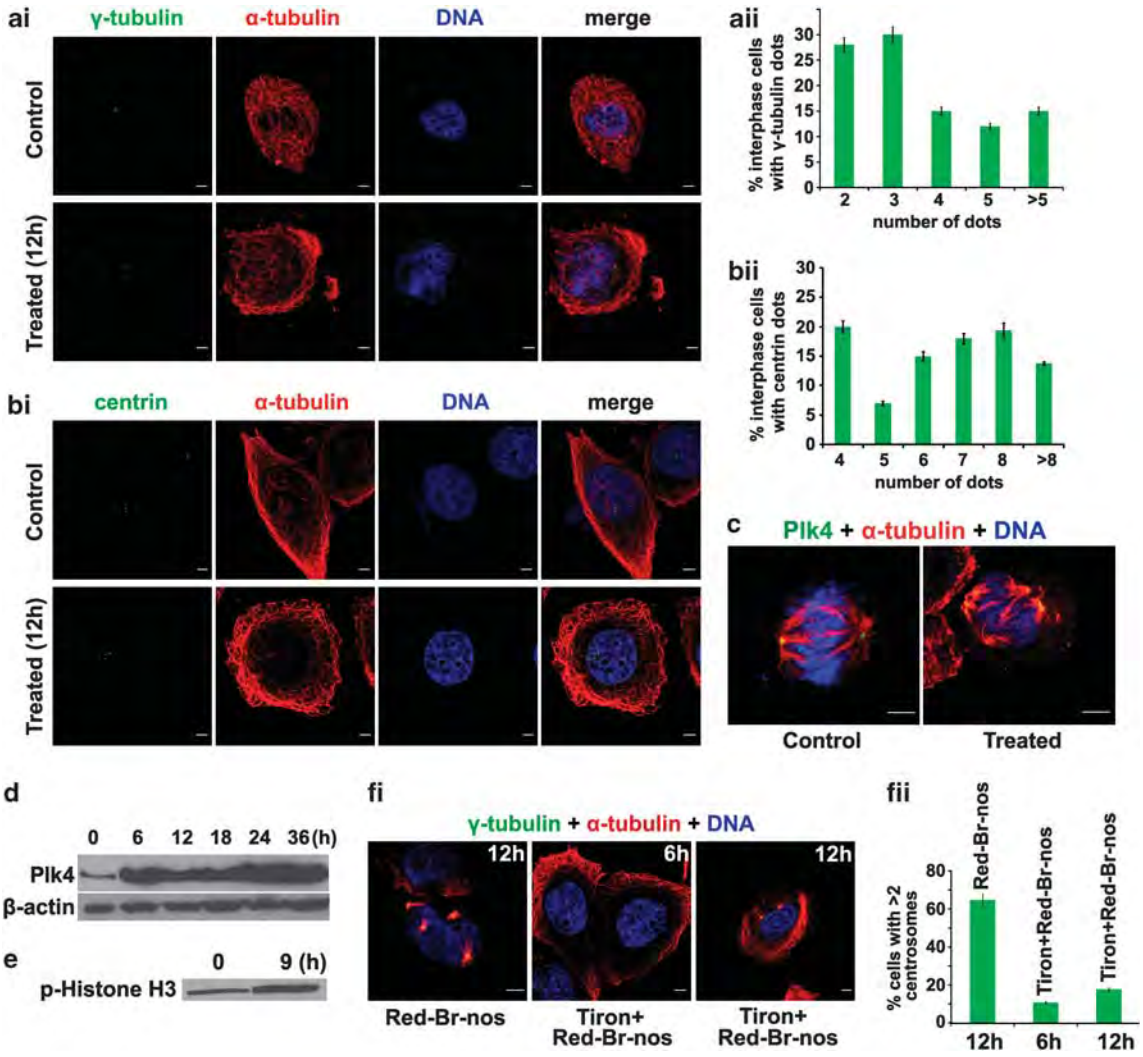

Figure 2 Red-Br-nos induces high-grade CA, which is ROS-dependent. (**ai** and **bi**) Immunofluorescence confocal micrographs of PC-3 cells treated with vehicle or Red-Br-nos (10 μM) for 12 h. Panels show γ-tubulin or centrin (green), MTs (red) and DNA (DAPI) in control (top row) and Red-Br-nos-treated (bottom row) interphase cells. (**aii** and **bii**) Bar-graph quantitation of the number of interphase PC-3 cells harboring the indicated number of γ-tubulin (upper) or centrin (lower) dots upon drug treatment. (**c**) Confocal immunomicrographs showing vehicle or drug-treated PC-3 cells stained for PLK4 (green), mictrotubules (red) and DNA (blue/DAPI). (**d**) Immunoblots showing PLK4 expression levels in PC-3 cells treated with 10 μM Red-Br-nos for the indicated times. β-actin was used as the loading control. (**e**) Immunoblot for phosphohistone-H3 showing increased kinase activity of cdk2 immunoprecipitated from 9-h Red-Br-nos-treated cells. (**fi**) Attenuation of ROS levels by 4-h tiron treatment followed by drug exposure for 6 and 12 h showed reduction in the incidence of cells harboring multiple centrosomes. γ-tubulin is in green, MTs in red and DNA in blue. (**fii**) Bar-graph quantitation shown. Scale bar = 5 μm

that this CA event is responsive to and downstream of DNA damage induced by ROS (Figures 2fi and ii). These data suggest that Red-Br-nos treatment causes upregulation of the centriolar biogenesis machinery and thus creates cytoplasmic conditions conducive to rapid centriolar assembly.

Red-Br-nos induces *de novo* CA. Having uncovered that Red-Br-nos induces robust CA, we focused our attention on deciphering the basis of this brisk CA. Given the increased proportion of cells with extensive CA within 9 h of drug treatment, 'templated' centrosome overduplication seemed an unlikely explanation. Thus, we sought to determine whether the amplified centrioles emerged *de novo* or through a 'templated' mechanism by centrosome overduplication. Because centriole maturation is an important functional property of the centriole, we immunostained drug-treated cells with cenexin, a specific marker for mature (mother) centrioles. The various mother-daughter combinations in both Red-Br-nos- and doxorubicin-treated PC-3 cells were visually scored using immunofluorescence microscopy (Figure 3). We did not observe a significant number of 'rosette-like' centrally positioned mother centrioles, and daughter centrioles appeared scattered throughout the cytosol far from mothers. Thus, we favor the idea that Red-Br-nos-induced CA is more likely to be an exceptional case of *de novo* centrosomal assembly occurring in presence of parent centrioles. This may be due to local accumulation of high concentration of centriolar material rather than concurrent formation of multiple daughters at the mother centriole. However, we found a few cells (~5%) wherein a

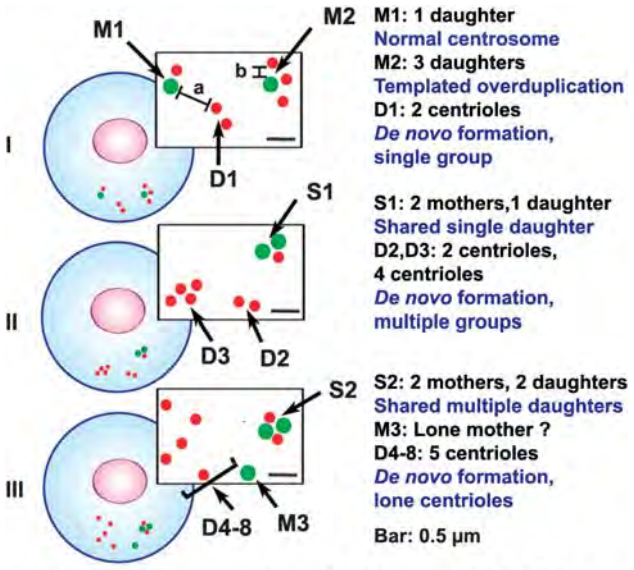

Figure 3 Schematic illustration of three representative cells depicting all the various mother–daughter centriole combinations that were observed upon Red-Br-nos or doxorubicin treatment. Cell I shows two mother centrioles (green), namely M1 and M2, and six daughter centrioles (red). M1 has one closely associated daughter ($<0.2\,\mu$m) and represents a 'normal' centrosome or is a result of a normal duplication event. M2 has three daughters lying in close vicinity ($\sim 0.2\,\mu$m) representing 'templated' overduplication. D1 refers to a *de novo*-formed pair of centrioles, because they are not associated with any mother ($>$ 0.2 μm). Cell II shows two mother centrioles (green) and seven daughter centrioles (red). S1 represents a 'shared' situation where a single daughter is shared between two mothers. We cannot exclude the possibility that the 'templated' or *de novo*-formed centrioles later mature to form mothers. D2 and D3 represent two separate clusters of *de novo* centrioles separated by a distance of $>0.2\,\mu$m. Cell III shows three mother centrioles (green) and seven daughter centrioles (red). S2 represents another shared situation where two daughters are shared between two mother centrioles. This situation could arise because of two successive rounds of duplication or may even represent a normal G2 situation. M3 represents a lone mother. D4–D8 represent *de novo* centrioles lying far apart from each other ($>0.2\,\mu$m)

single maternal centriole concurrently generated multiple daughter centrioles, as seen by a 'rosette-like' pattern of one cenexin-positive mother centriole surrounded by several centrin-positive daughters (Figure 4Ai, panel bv). Overall, a significant increase in cells with more than one daughter per maternal centriole was observed. Red-Br-nos-induced *de novo* centriolar assembly is particularly intriguing given that nocodazole, which disassembles MTs, actually prevents *de novo* centriole formation.[32] This may be ascribed to the 'gentler' MT-modulating effects of Red-Br-nos, which does not alter the monomer/polymer ratio of tubulin even at high concentrations.[16] Although Red-Br-nos binds soluble tubulin as evidenced by kinetic quenching of intrinsic tryptophan fluorescence of tubulin (Supplementary Figure 2A), a concentration of up to 200 μM did not induce significant structural damage to tubulin as indicated by an absence of change in 1-anilinonaphthalene-8-sulfonic acid-tubulin fluorescence upon addition of Red-Br-nos (Supplementary Figure 2B). Instead, it seems that Red-Br-nos binds 'gently' to tubulin, which results in attenuated MT dynamics rather than drastic de- or overpolymerization. This attribute perhaps distinguishes Red-Br-nos from other MT-interfering drugs that exert structural damage to MTs. The CA induced by Red-Br-nos also distinguishes it from other conventional chemotherapeutics that cause CA. For instance, doxorubicin, a DNA-intercalating drug, induces CA with a nominal daughter (cenexin-negative) to mother (cenexin-positive) ratio (Figure 4B). This observation suggests that CA occurs by several rounds of duplication resulting in numerous mother centrioles with extra daughter centrioles, perhaps during an enhanced cell-cycle arrest. Because daughter centrioles are held close to their mother by a linker[33] unlike *de novo* centrioles, scoring was based on physical distance between mother and daughter centrioles for all observed patterns (Figure 3). A physical distance of $\leq 0.2\,\mu$m between mother and daughter centriole was categorized as 'templated', whereas a distance $>0.2\,\mu$m was considered *de novo*. Visual observations of the number of 'templated' *versus de novo* centrioles, in 150 cells each, were recorded in a simple database. This allowed us to detect trends and statistically quantify and compare numerical centriole aberrations in Red-Br-nos- and doxorubicin-treated cells. Databases for both Red-Br-nos and doxorubicin were queried to address number of cells containing: (a) no *de novo* daughters; (b) a daughter: mother ratio ≥ 2; (c) ≤ 2 mothers (i.e., cells with no instance of CA resulting from several rounds of duplication); and (d) at least one mother with >1 daughter (i.e., cells with at least one instance of 'templated' overduplication). Our first database query (a) to uncover the percentage of cells with an absence of *de novo* centrioles yielded a significantly higher proportion of cells devoid of *de novo* centrioles upon doxorubicin treatment compared with Red-Br-nos (126 cells with no *de novo* centrioles upon doxorubicin treatment compared with only 12 in Red-Br-nos-treated cells, out of 150 cells). Our next query (b) revealed a significant number of cells bearing a very high ratio of daughter:mother (≥ 2) upon Red-Br-nos treatment as compared with doxorubicin. A search for cells having ≤ 2 mother centrioles revealed that there were more instances of CA resulting from several rounds of centrosome-duplication cycle following doxorubicin *versus* Red-Br-nos treatment. Lastly, querying for cells harboring at least one mother associated with more than one daughter (daughters at a distance closer than 0.2 μm) yielded a higher number of cells showing 'templated' overduplication for doxorubicin (107/150 doxorubicin-treated cells *versus* 68/150 Red-Br-nos-treated cells) These analyses suggest a spatially more restricted or 'templated' pattern of centriole overduplication in case of doxorubicin, which is compromised by Red-Br-nos (Figure 4Ci). We further compared the extent of *de novo* centriole formation in cells exhibiting 'normal-like' CA consequent to multiple rounds of duplication with 'templated' CA events. The number of *de novo* centrioles was counted in the output of queries (c) and (d) for both Red-Br-nos- and doxorubicin-treated cells. The average number of *de novo* centrioles was plotted as shown in Figures 4Cii and iii. We found that the average number of *de novo* centrioles was much higher with Red-Br-nos, irrespective of 'templated' overduplication. Collectively, these data suggest the occurrence of more extensive *de novo* centriolar formation in Red-Br-nos-treated cells compared with doxorubicin.

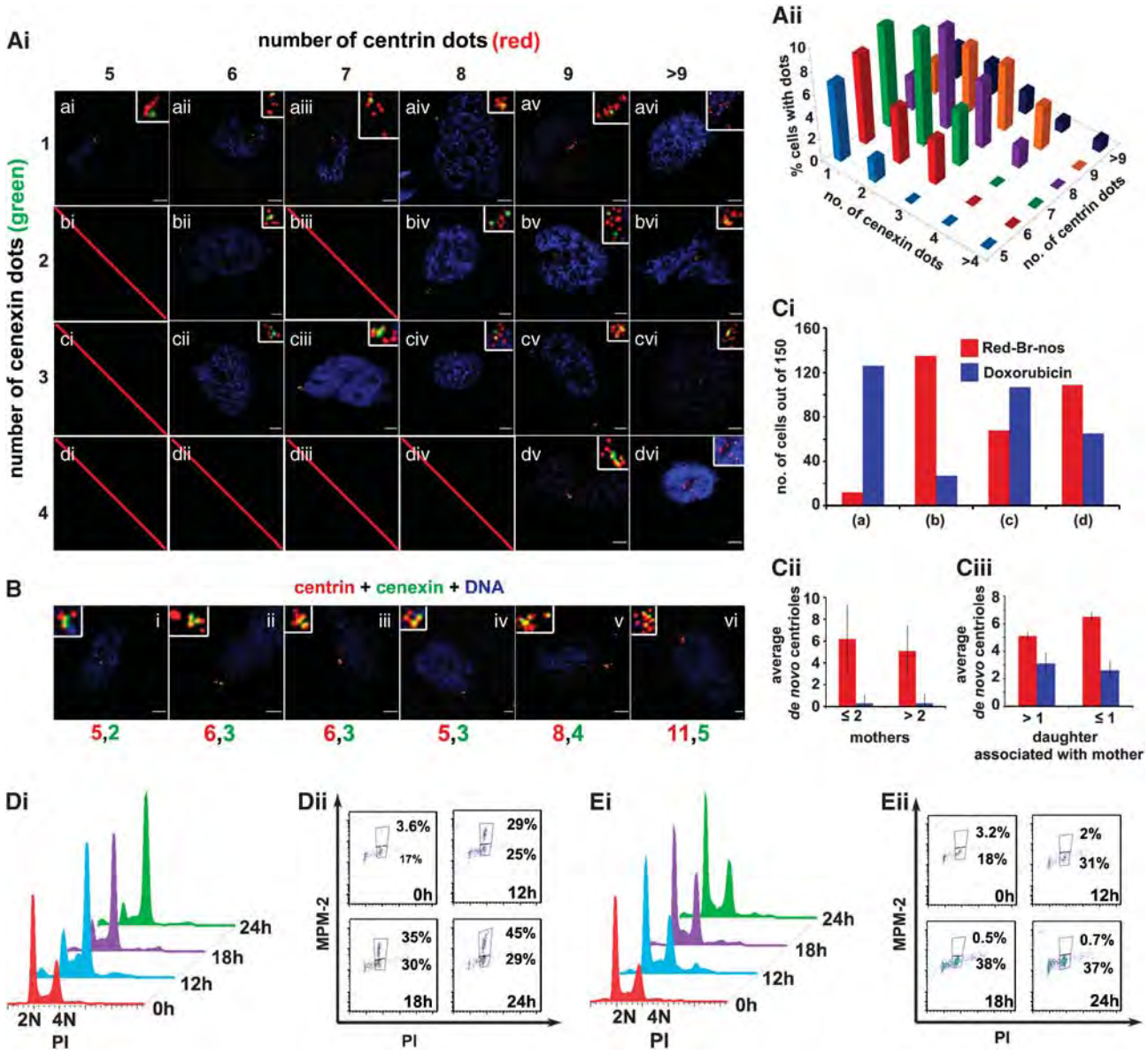

Figure 4 Unlike doxorubicin, Red-Br-nos causes *de novo* centriole formation and mitotic arrest in PC-3 cells. (**Ai**) Immunofluorescence confocal micrographs showing various permutations of centrin (daughter) and cenexin (mother) dots in Red-Br-nos-treated (10 μM for 18 h) PC-3 cells. Centrin is shown in red, cenexin in green and DNA in blue. (**Aii**) Three-dimensional bar-graph plot representing the percent cell population with specified patterns of centrin and cenexin dots. (**b**) Confocal immunomicrographs showing cells with various permutations and combinations of centrin (daughter) and cenexin (mother) dots in doxorubicin-treated (10 μM for 18 h) PC-3 cells. Centrin is shown in red, cenexin in green and DNA in blue. (**Ci**) Bar graph depicting the outcomes of our database queries on cells treated with either Red-Br-nos (10 μM) or doxorubicin (10 μM) for 18 h. (a), (b), (c) and (d) refer to the database search queries. (a) is the number of cells with an absence of *de novo* centrioles, (b) represents the number of cells where ratio of daughters to mothers is ≥ 2, (c) represents cells with ≤ 2 mothers, signifying cells lacking amplification due to several rounds of duplication and (d) represents cells with at least one mother associated with more than one spatially close daughter. A total of 150 cells were analyzed in each case. (**Cii**) The output of query (c) that resulted in number of cells with at least one instance of 'templated' amplification upon multiple rounds of duplication was further analyzed for average number of *de novo* centrioles as shown in bar graph. (**Ciii**) The output of query (d) resulted in the number of cells exhibiting 'templated' duplication that were further analyzed for number of *de novo* centrioles as plotted in bar graph. (**Di** and **Ei**) Three-dimensional DNA histograms representing cell-cycle kinetics of PC-3 cells treated with Red-Br-nos (10 μM) or doxorubicin (10 μM), respectively. The X-axis shows DNA amounts representing different cell-cycle phases, the Y-axis shows the number of cells containing that amount of DNA and the Z-axis shows the duration of treatment. (**Dii** and **Eii**) Corresponding dual-color dot plots showing the proportion of mitotic cells (MPM-2-positive) as opposed to G2 cells (MPM-2-negative). Scale bar = 5 μm

Red-Br-nos abrogates DNA-damage-induced G2 checkpoint leading to mitotic entry. In normal cells, S and G2/M checkpoints prevent cells with incompletely replicated or damaged DNA from entering mitosis. However, cancer cells possess compromised checkpoints and cell-cycle arrest due to DNA damage may be weak and relatively easy to breach. Anticancer drugs that exacerbate DNA damage and inactivate the G2 checkpoint to induce apoptosis can capitalize on this Achilles' heel of cancer cells.[34] Thus, we next explored whether PC-3 cells that suffered DNA damage upon

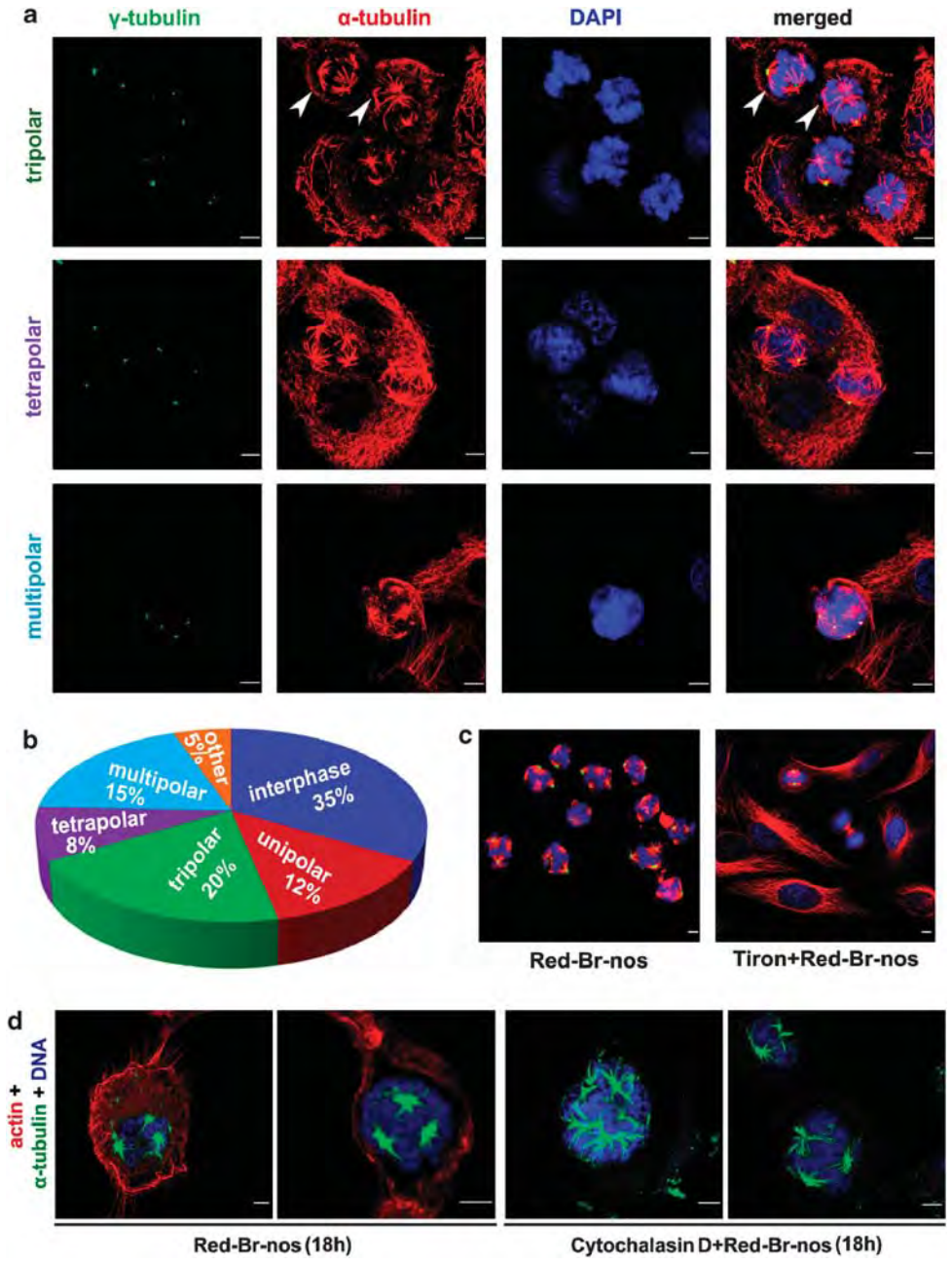

Figure 5 Red-Br-nos induces high-grade SM in PC-3 cells. (**a**) Immunofluorescence confocal micrographs of PC-3 cells 'stuck' in mitosis upon treatment with Red-Br-nos (10 μM) for 18 h. Panels show γ-tubulin in green, MTs in red and DNA in blue (DAPI). (**b**) Pie-chart quantitation of the proportion of cells exhibiting specified spindle polarity. The category classified as 'other' predominantly includes bipolar mitotic cells or cells exhibiting aneuploidy and 'mitotic catastrophe'. (**c**) ROS inhibition by tiron treatment preceding Red-Br-nos treatment (10 μM) for 24 h showed reduced multipolarity as compared with Red-Br-nos treatment alone. Mictrotubules are shown in red and DNA in blue. (**d**) PC-3 cells pretreated with cytochalasin D (1 μM) for 4 h and then treated with Red-Br-nos for 18 h showed enhanced spindle-pole amplification as compared with only Red-Br-nos treatment (10 μM) for 18 h. Actin is shown in red, MTs in green and DNA in blue. Scale bar = 5 μm

Red-Br-nos treatment stalled in S or G2 phase or entered mitosis. We performed a flow-cytometric analysis to investigate how Red-Br-nos affects cell-cycle phases over time. We found that Red-Br-nos did not induce obvious S or G2 arrest, instead, cells slowly progressed through S and G2 and entered mitosis with damaged DNA (Figures 4Di and ii). About 25% of PC-3 cells were in mitosis as early as 12 h, and mitotic index peaked at 24 h post treatment. This suggested that Red-Br-nos efficiently mediated abrogation of G2/M checkpoint, causing cells to enter mitosis despite compromised DNA integrity. Moreover, Red-Br-nos induced *de novo* centrosomes appeared functionally competent as MT-organizing centers because they efficiently orchestrated multipolar spindle assembly.

For the cell-cycle data as well, we based our comparisons of Red-Br-nos to doxorubicin. Unlike Red-Br-nos,

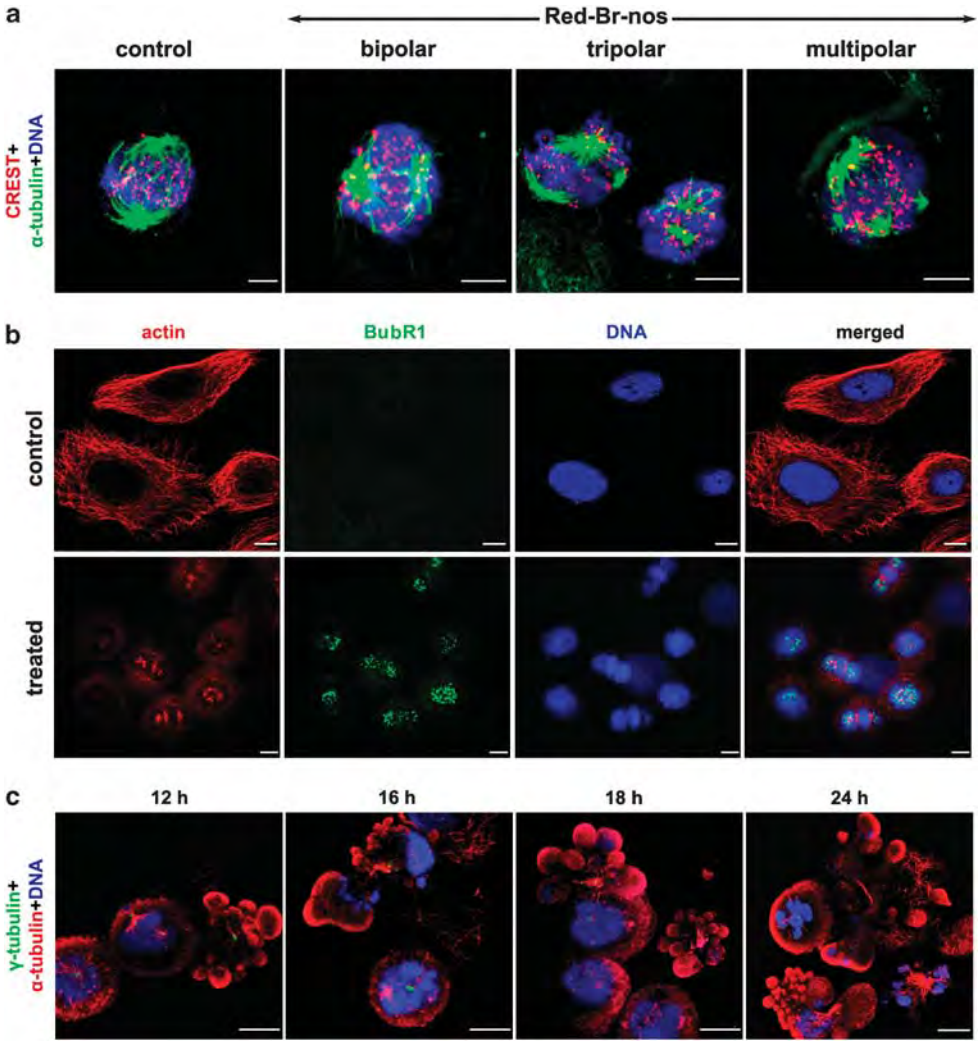

Figure 6 Red-Br-nos activates the SAC and induces 'metaphase catastrophe'. (**a**) Immunomicrographs showing PC-3 cells treated with vehicle or Red-Br-nos (10 μM) for 18 h and stained for kinetochores with CREST (red), MTs with α-tubulin (green) and DNA with DAPI (blue). (**b**) Panels show BuBR1- (green), actin- (red) and DNA- (blue) stained PC-3 cells treated with vehicle (top panel) or Red-Br-nos (lower panel) for 9 h. (**c**) Immunofluorescence confocal micrographs representing 'mitotic catastrophe' upon Red-Br-nos treatment at the specified time points. Multipolar cells with membrane blebs or protrusions rich in α-tubulin were indicative of cells dying following an unsuccessful metaphase. γ-tubulin is shown in green, α-tubulin in red and DNA in blue. Scale bar = 10 μm

doxorubicin-treated PC-3 cells showed a chronic S/G2 arrest at 12 h and the cells stayed in G2 for over 24 h (Figures 4Ei and ii). During this durable S/G2 arrest, rampant CA became evident. Interestingly, doxorubicin-treated cells with extra centrosomes did not show a high ratio of centrin to cenexin spots. In addition, daughter centrioles appeared closely associated with mother centrioles. These observations were more consonant with multiple cycles of 'templated' duplication rather than *de novo* centrosome formation. Intriguingly, doxorubicin-treated cells were chronically 'stuck' in G2 and failed to enter mitosis even 28 h post treatment. This phenotype stood in stark contrast to that of Red-Br-nos-treated cells, which were transiently arrested in G2 and abrogated the G2/M checkpoint to enter mitosis as early as 12 h post treatment. Taken together, these data suggest that Red-Br-nos-induced CA occurs via *de novo* biogenesis that differs qualitatively from 'templated' centriole duplication observed following doxorubicin exposure.

CA induces rampant mitotic SM by persistent centrosome declustering. We next quantitated the number of centrosomes per pole in mitotic cells upon Red-Br-nos treatment using immunofluorescence confocal microscopy. In control cells, all cell-cycle stages appeared normal and mitotic cells exhibited typical bipolar spindles at the expected frequency (Supplementary Figure 3). However, 18 h Red-Br-nos-treated cells showed a preponderance of multipolar spindles with defects in chromosome congression to metaphase plate (Figure 5a). Quantitation of unipolar, bipolar, tripolar, tetrapolar and multipolar ($n>4$, $n=$number of spindle poles per cell) spindles is shown in Figure 5b. Intriguingly, we found that the multipolar phenotype progressively increased over time (Supplementary Figure 4), indicating persistent centrosome declustering. Most spindle poles in a multipolar configuration showed presence of 'real' centrioles ($\sim$80%, $n=200$), confirming robust CA.

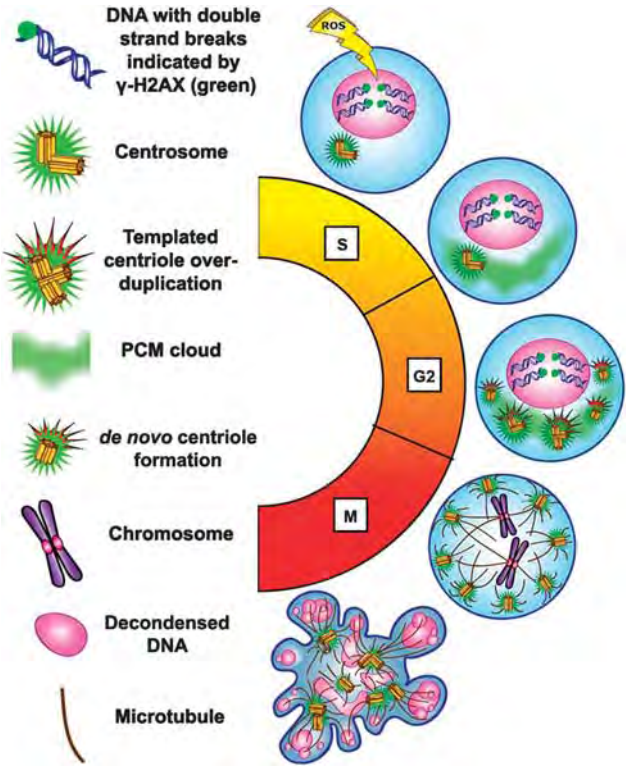

Figure 7 Schematic illustration of a proposed model depicting the progression of events upon induction of high ROS levels by Red-Br-nos. High-grade DNA damage results in transient S/G2 arrest (depicted in yellow/orange) followed by a chronic mitotic arrest (depicted in red). Accumulation of S-phase-specific cyclins/cdks results in accrual of PCM components in the vicinity of an already existing and 'ready to duplicate' centrosome. CA, predominantly *de novo* centriole formation along with some degree of 'templated' overduplication, occurs during the transient S/G2 arrest, which then translates into excessively multipolar phenotypes during a stalled mitosis. Majority of the arrested multipolar cells succumb to 'metaphase catastrophe' due to the chaos arising from multiple insults the cells have suffered including irreparable DNA damage, aberrant kinetochore-MT attachments and spindle multipolarity

Having observed ROS-dependent DNA damage that perhaps resulted in CA-driven SM, we were curious to determine whether attenuation of ROS levels affected the severity of spindle-pole amplification during mitosis. To this end, we pretreated cells with tiron for 4 h before Red-Br-nos exposure for 18 h. Our results showed that attenuation of ROS levels with tiron reduced the multipolar phenotype in cells (Figure 5c), perhaps due to a decline in the severity of ROS-induced DNA damage that translated into CA. However, for reasons yet obscure, we also observed an overall decrease in number of mitotic cells with tiron treatment. The mitotic index was assessed using MPM-2, a mitosis-specific marker in a dual-color flow-cytometric experiment. MPM-2-negative cells with 4 N DNA were considered as G2, whereas MPM-2-positive/4 N DNA cells were read as mitotic. The mitotic population in Red-Br-nos-treated cells at 24 h was ~60%, which dropped to ~10% in 4 h tiron-pretreated cells that were drug-treated for 24 h (data not shown).

We next examined whether formation of multipolar spindles depended on cytoskeletal actin. To this end, cells were treated with cytochalasin D for 4 h followed by a 12-h Red-Br-nos exposure. We found that multipolar spindles with 'real' centrioles were retained in presence of cytochalasin D, suggesting that SM was independent of actin filaments (Figure 5d). Surprisingly, cytochalasin treatment increased number of spindle poles. We speculate that disruption of actin-based centrosome clustering mechanisms (involving interactions of astral MTs with cortical actin) may have enhanced centrosome declustering.[35,36]

Red-Br-nos activates spindle-assembly checkpoint (SAC) and induces 'metaphase catastrophe'. Having identified rampant spindle-pole amplification upon Red-Br-nos treatment, we wondered if MTs emanating from poles were able to attach properly to kinetochores. Essentially, establishment of optimal sister kinetochore tension is necessary to silence the 'wait anaphase' signal of the SAC. As expected, red kinetochore dots across sister kinetochores did not 'line up' owing to the presence of aberrant spindle morphology (Figure 6a). These unattached or misaligned kinetochores may underlie SAC activation as seen by intense BubR1 staining in drug-treated cells (Figure 6b). This observation suggests that lack of tension and/or existence of aberrant kinetochore-MT attachments underlie SAC activation.

As the aberrant multipolar configuration of cells cannot exist indefinitely, we next evaluated the long-term fate of Red-Br-nos-treated mitotically arrested cells. We determined whether mitotic cells with multipolar spindles directly succumb to cell death, which we refer to as 'metaphase catastrophe,' or progress to an abnormal anaphase and proceed through aberrant cytokinesis to result in multiple daughters, recently referred to as 'anaphase catastrophe'.[12] Our immunofluorescence microscopy data showed that a large percentage of mitotic cells (~70%) eventually underwent metaphase catastrophe (Figure 6c). Protrusions of tubulin-rich cellular membrane were evident and indicated commencement of apoptosis, perhaps marking a 'point of no return'. We propose that the process of 'metaphase catastrophe' is distinct from 'anaphase catastrophe'. We found that metaphase cell death was accompanied by extensive membrane blebbing, which was not suppressed by z-vad-fmk, suggesting caspase-independent apoptosis (data not shown). However, a few 'metaphase-catastrophe refractory' cells underwent aberrant anaphase to yield ~5% incidence of 'anaphase catastrophe'. Such cells progressed through mitosis with multiple lobes followed by a complete or incomplete cytokinesis.

Discussion

CA has long been considered as a hallmark of cancer.[4] Although CA allows maintenance of 'optimal' aneuploidy to facilitate tumorigenesis by selection of karyotypes that offer growth advantage,[38] exacerbation of CA may be detrimental to cancer cell survival, thus serving as a favorable chemotherapeutic approach. Essentially, robust CA generates aberrant mitotic spindles with chromosomes migrating to numerous poles, hence causing aneuploidy. Depending upon the degree of aneuploidy, it may be tumor- or death-promoting.[39] Our current study demonstrates for the first time a link between Red-Br-nos-induced early ROS production and DNA damage

with CA-induced SM, which formed the basis of substantial cell death via 'metaphase catastrophe' (Figure 7).

Several reports detail four accepted models of CA etiology,[40] including CA resulting from centrosome-nuclear cycle uncoupling,[41,42] cytokinesis failure,[43] cell–cell fusion,[44] and DNA damage (which actually may simply represent centrosome fragmentation).[27] Our data demonstrate that Red-Br-nos-induced CA begins in S phase and continues robustly during the ephemeral G2 arrest. Finally, cells override the G2 checkpoint and enter mitosis in which they succumb to 'metaphase catastrophe'. Although ATR activation is known to promote recovery of collapsed replication forks, and thus should result in considerable S/G2-phase arrest, this does not seem to be the case. It has been shown that ATR-induced S-phase arrest acts mainly through the p53-dependent pathway.[45,46] Because PC-3 cells are p53-negative,[47] despite presence of extensive and severe ROS-induced DNA damage, flow-cytometric analysis indicated only a transient S-phase arrest, suggesting that the observed CA was not accompanied by prolonged S-phase stall. Furthermore, Red-Br-nos caused a loss of the strict correlation between number of centrioles and ploidy, which was clearly not a consequence of failed cytokinesis because a majority of treated cells perished much earlier, that is, in metaphase. Thus, our observations supplement current models by adding a novel mode of CA. This is in addition to our previous observations that showed autophagy (as seen by LC3-II) induction in PC-3 cells treated with Red-Br-nos at 25 μM[19] and even lower doses of 10 μM (Supplementary Figure 6A). These data collectively suggest the concurrent induction of ROS-mediated CA and the autophagic pathways that lead to cell death.

Induction of CA by Red-Br-nos shows the following distinctive characteristics: (a) generation of 3–8 centrosomes per cell, (b) ratio of daughter to mother centrioles >1 (i.e., greater than expected for 'templated' duplication) and (c) rapid and efficient production of several centrioles in parallel within 9–12 h of drug exposure. Normally, in each individual cell cycle, only one new centrosome is duplicated, close to the preexisting organelle via a semi-conservative 'templated' mechanism. In contrast, the canonical description of *de novo* centriole formation encompasses two key features: (1) it occurs in the absence of preexisting centrioles and (2) the process is slower than normal centriole duplication. Recently, though, the line demarcating normal duplication, 'templated' overduplication and *de novo* centriole formation has blurred.[48] There is speculation ablaze that normal procentriole formation is potentially a type of *de novo* centriole assembly, only restricted spatially and numerically and hence more tightly regulated.[48] This regulation is orchestrated by the mother centriole that enriches the PCM with centriole biogenesis factors and concentrates the PCM to define the number as well as the proximity of emerging procentrioles.[49] This configuration is then 'locked' by linker proteins between mother and procentriole, thus suppressing formation of superfluous daughter centrioles. There are some examples of *de novo* centrosome formation in nature, for example, in clam zygotes,[50] mice[51,52] and rabbit blastomeres.[53] These instances occur in the absence of a preexisting organelle and early in development, when large reserves of maternal products for centriole formation are stored in the oocyte. Also, *de novo* formation of centrioles occurs exclusively in S phase in *Chlamydomonas*,[54] and the duplication efficiency is only half that of 'templated' assembly. A seminal study demonstrating *de novo* centrosome formation utilized S--phase-arrested cells in which the existing centrosome was destroyed by laser ablation, bolstering the notion that *de novo* centriole formation can only occur in the absence of the parent centrosome.[32] In this study, *de novo* induction of centriole biogenesis was a slow process beginning only about 5–8 h after centrosome ablation and requiring almost 24 h for completion.[32]

We found that Red-Br-nos treatment causes rapid and simultaneous production of multiple centrosomes scattered throughout the cytoplasm in the presence of the original centrosome. Evidently, the mother centrosome is failing to spatially restrict procentriole formation to its vicinity and thus cannot limit the number of new procentrioles to one per mother. This could be analogous to having no mother centriole at all (a canonical characteristic of *de novo* formation). We believe that by causing a surge in levels of structural or regulatory components (PLK4 and cdk2) of the centriolar biogenesis machinery that are normally rate-limiting, Red-Br-nos pushes the centrosome-duplication machinery into overdrive. The unique intracellular environment thus created would account for the accelerated and efficient production of centrioles throughout the cytoplasm. This intracellular state is different from that in studies involving laser centrosome ablation and may account for the unusual briskness in *de novo* centriole formation upon Red-Br-nos treatment. PLK4 overexpression causes concomitant formation of multiple daughter centrioles in a 'rosette' configuration around a single maternal centriole,[31,55] which we observed in rare instances. Thus, both the pathways of *de novo* formation and (albeit to a much smaller extent) 'templated' overduplication are activated upon Red-Br-nos treatment leading to a 'centrosome overload'. Our observations thus concur with the diminishing lines separating the different CA pathways and support the hypothesis that the 'templated' mechanism for centriole replication is needed, not because the *de novo* pathway is inefficient, but rather because it sets limits on the number of centrioles produced during each individual cell cycle.[56]

We believe that Red-Br-nos displays several features that set it apart from conventional DNA-damaging drugs. Unlike doxorubicin, which causes CA during a chronic S-phase arrest, Red-Br-nos forces cells to transit through S phase and subsequently override the transient G2/M arrest to progress into mitosis despite DNA damage, although they eventually die via 'metaphase catastrophe'. Thus, Red-Br-nos distinguishes itself from other traditional DNA-damaging agents, although it does act similar to UCN-01.[34] Moreover, it has been shown that DNA-damage-induced cell death is enhanced by progression through mitosis,[20] a conclusion which is corroborated by our observations.

Intriguingly, a slight structural alteration (reduction of the lactone ring to a cyclic ether) of Red-Br-nos compared with noscapine and its congener, bromonoscapine, remarkably intensifies CA and drives SM and 'metaphase catastrophe'. Presumably, the power of Red-Br-nos to amplify centrosomes

and cause multipolarity translates into superior chemotherapeutic strength, as a recent NCI screen revealed that Red-Br-nos is significantly more potent than noscapine in virtually all cancer lines tested (Supplementary Figure 5). Nonetheless, Red-Br-nos retains the non-toxic attributes of the mildly declustering parent, noscapine, and spares normal cells.[18] This is perhaps because normal cells, owing to robust checkpoints, have durable mechanisms that prevent cell-cycle progression in the presence of damaged DNA. In contrast, cancer cells have leaky checkpoints, which they invoke but fail to sustain, and thus march through the cell cycle with lethal consequences. Red-Br-nos-induced downmodulation of MT dynamicity in healthy cells may be harmless because normal checkpoint systems mitigate the impact. In contrast, cancer cells may 'ignore' the impairment to their detriment. We speculate that the leakiness of cancer cell checkpoints combined with the mild impact of Red-Br-nos on MT dynamicity constitute the basis of its cancer cell selectivity and nontoxicity, respectively. We are optimistic that Red-Br-nos can serve as an invaluable tool to gain insights into *de novo* centriole formation and molecular mechanisms that normally restrict centriole numbers.

Materials and Methods

Cell lines, culture and drug treatment. PC-3 cells were grown in RPMI medium supplemented with 10% fetal bovine serum and 1% penicillin/streptomycin. Red-Br-nos was synthesized from noscapine as described previously in the Supplementary Data section (Supplementary Scheme 1). Stock solutions of 50 mM were prepared in DMSO and kept frozen at $-20\,^{\circ}C$ until use. All Red-Br-nos treatments were done at 10 μM concentration for the indicated time points. Tiron was used at 1 mM concentration.

Kinase activity assay. To examine cdk2 kinase activity, cdk2 antibody was used to selectively immunoprecipitate cdk2 from vehicle- and Red-Br-nos-treated PC-3 cell lysates. The resulting immunoprecipitate was incubated with pure histone-H3 protein in the presence of ATP and kinase buffer. The kinase assay reaction allowed immunoprecipitated cdk2 to phosphorylate histone-H3 *in vitro*, the extent of which was measured by immunoblotting using phosphohistone-H3 antibody from Cell Signaling (Beverly, MA, USA). Histone-H3 protein was from Millipore (Billerica, MA, USA) and ATP was from Cell Signaling.

Immunofluorescence microscopy, cell-cycle analysis and immunoblotting. Cells were cultured to $\sim$70% confluence and medium was replaced with fresh medium containing either vehicle (0.1% DMSO) or 10 μM Red-Br-nos for the noted times, followed by processing for immunofluorescence microcopy, flow cytometry or immunoblotting as described previously.[6,13,19] Mitotic index was determined by using mitotic protein monoclonal-2 (MPM-2) antibody from Cell Signaling as described previously.[19] Antibodies against γ-tubulin, α-tubulin and β-actin were from Sigma (St. Louis, MO, USA). Anti-BubR1 antibody was from BD Biosciences (Pharmingen, San Jose, CA, USA) and human anti-centromere ACA antibody for kinetochore staining was from Antibodies, Inc. (Davis, CA, USA). Antibodies for γ-H2AX, PLK4, p-bcl2, p-ATR and p-chk1 were from Cell Signaling. Cenexin antibody was a generous gift from Dr. Stephen Doxsey, University of Massachusetts (Worcester, MA, USA). Alexa 488- or 555- conjugated secondary antibodies were from Invitrogen (Carlsbad, CA, USA). Horseradish peroxidase-conjugated secondary antibodies were from Santa Cruz Biotechnology (Santa Cruz, CA, USA). Detailed analysis of γ-H2AX immunofluorescence signal intensity was performed utilizing Metamorph analysis software (Molecular Devices, Sunnyvale, CA, USA). The final output for both vehicle- and Red-Br-nos-treated cells was the integrated intensity based on total stained area and staining intensity at individual pixels. Cell-cycle profiling was done on LSRFortessa flow-cytometer (BD Biosciences) and analyzed using Flowjo software (Tree Star, Ashland, OR, USA).

Database search method for the numerical analysis of centrioles. Observations of the number of 'templated' *versus de novo* centrioles were recorded in a simple database in the following manner. Each cell studied was allocated a unique identification number (cell ID). For each cell ID, there were zero or more mother centrioles present. Each was given a unique identification number (mother ID) for that cell and labeled M1, M2 and so on. For each mother ID, the number of associated daughter centrioles was recorded. Additionally, zero or more isolated *de novo* groups of centrioles may be present for the cell. For each such group present, a unique identification number was allocated and labeled D1, D2 and so on. For each *de novo* group ID, the number of associated daughters was recorded. In a similar manner, any daughters shared by two mothers (there was no instance of more than two mothers sharing daughters) were recorded with labels S1, S2 and so on. Complete records for two successive cells as it appeared in the database are represented by data in Supplementary Table 1. Two databases were created by reading a comma-separated list of records into a simple program written in the Python programming language, specifically designed for these data. One database contained 150 cells of *[TYPE_A_Rd-Br-nos]* and the other contained 150 cells of *[TYPE_B_Doxo]*. The databases were each searched for a total of four queries as discussed in the Results section as well as in the legend to Figure 3.

Statistical analysis. All experiments were repeated three times. Data were expressed as mean $\pm$ S.D. Statistical analysis was performed using Student's *t*-test. The criterion for statistical significance was $P<0.05$.

Conflict of Interest

The authors declare no conflict of interest.

Acknowledgements. We thank Professor Leslie Wilson (University of California, Santa Barbara) for the support with spectrofluorimetric experiments. This work was supported by grants to RA from the National Cancer Institute at the National Institutes of Health (1R00CA131489).

1. Lingle WL, Lukasiewicz K, Salisbury JL. Deregulation of the centrosome cycle and the origin of chromosomal instability in cancer. *Adv Exp Med Biol* 2005; **570**: 393–421.
2. Holland AJ, Cleveland DW. Boveri revisited: chromosomal instability, aneuploidy and tumorigenesis. *Nat Rev Mol Cell Biol* 2009; **10**: 478–487.
3. Brinkley BR. Managing the centrosome numbers game: from chaos to stability in cancer cell division. *Trends Cell Biol* 2001; **11**: 18–21.
4. Quintyne NJ, Reing JE, Hoffelder DR, Gollin SM, Saunders WS. Spindle multipolarity is prevented by centrosomal clustering. *Science* 2005; **307**: 127–129.
5. Ganem NJ, Godinho SA, Pellman D. A mechanism linking extra centrosomes to chromosomal instability. *Nature* 2009; **460**: 278–282.
6. Karna P, Rida PC, Pannu V, Gupta KK, Dalton WB, Joshi H *et al.* A novel microtubule-modulating noscapinoid triggers apoptosis by inducing spindle multipolarity via centrosome amplification and declustering. *Cell Death Differ* 2011; **18**: 632–644.
7. Godinho SA, Kwon M, Pellman D. Centrosomes and cancer: how cancer cells divide with too many centrosomes. *Cancer Metastasis Rev* 2009; **28**: 85–98.
8. Boonstra J, Post JA. Molecular events associated with reactive oxygen species and cell-cycle progression in mammalian cells. *Gene* 2004; **337**: 1–13.
9. Burhans WC, Heintz NH. The cell-cycle is a redox cycle: linking phase-specific targets to cell fate. *Free Radic Biol Med* 2009; **47**: 1282–1293.
10. Loffler H, Lukas J, Bartek J, Kramer A. Structure meets function—centrosomes, genome maintenance and the DNA-damage response. *Exp Cell Res* 2006; **312**: 2633–2640.
11. Doxsey SJ. Centrosomes as command centres for cellular control. *Nat Cell Biol* 2001; **3**: E105–E108.
12. Galimberti F, Thompson SL, Ravi S, Compton DA, Dmitrovsky E. Anaphase catastrophe is a target for cancer therapy. *Clin Cancer Res* 2011; **17**: 1218–1222.
13. Aneja R, Lopus M, Zhou J, Vangapandu SN, Ghaleb A, Yao J *et al.* Rational design of the microtubule-targeting anti-breast cancer drug EM015. *Cancer Res* 2006; **66**: 3782–3791.
14. Aneja R, Zhou J, Vangapandu SN, Zhou B, Chandra R, Joshi HC. Drug-resistant T-lymphoid tumors undergo apoptosis selectively in response to an antimicrotubule agent, EM011. *Blood* 2006; **107**: 2486–2492.
15. Mishra RC, Karna P, Gundala SR, Pannu V, Stanton RA, Gupta KK *et al.* Second generation benzofuranone ring substituted noscapine analogs: synthesis and biological evaluation. *Biochem Pharmacol* 2011; **82**: 110–121.
16. Zhou J, Gupta K, Aggarwal S, Aneja R, Chandra R, Panda D *et al.* Brominated derivatives of noscapine are potent microtubule-interfering agents that perturb mitosis and inhibit cell proliferation. *Mol Pharmacol* 2003; **63**: 799–807.
17. Landen JW, Lang R, McMahon SJ, Rusan NM, Yvon AM, Adams AW *et al.* Noscapine alters microtubule dynamics in living cells and inhibits the progression of melanoma. *Cancer Res* 2002; **62**: 4109–4114.

18. Zhou J, Liu M, Luthra R, Jones J, Aneja R, Chandra R *et al.* EM012, a microtubule-interfering agent, inhibits the progression of multidrug-resistant human ovarian cancer both in cultured cells and in athymic nude mice. *Cancer Chemother Pharmacol* 2005; **55**: 461–465.
19. Karna P, Zughaier S, Pannu V, Simmons R, Narayan S, Aneja R. Induction of reactive oxygen species-mediated autophagy by a novel microtubule-modulating agent. *J Biol Chem* 2010; **285**: 18737–18748.
20. Varmark H, Sparks CA, Nordberg JJ, Koppetsch BS, Theurkauf WE. DNA-damage-induced cell death is enhanced by progression through mitosis. *Cell Cycle* 2009; **8**: 2951–2963.
21. Dodson H, Bourke E, Jeffers LJ, Vagnarelli P, Sonoda E, Takeda S *et al.* Centrosome amplification induced by DNA-damage occurs during a prolonged G2 phase and involves ATM. *EMBO J* 2004; **23**: 3864–3873.
22. Bartek J, J Lukas. Chk1 and Chk2 kinases in checkpoint control and cancer. *Cancer Cell* 2003; **3**: 421–429.
23. Yang J, Su Y, Richmond A. Antioxidants tiron and *N*-acetyl-L-cysteine differentially mediate apoptosis in melanoma cells via a reactive oxygen species-independent NF-kappaB pathway. *Free Radic Biolo Med* 2007; **42**: 1369–1380.
24. Kim JS, Cho EW, Chung HW, Kim IG. Effects of tiron, 4,5-dihydroxy-1,3-benzene disulfonic acid, on human promyelotic HL-60 leukemia cell differentiation and death. *Toxicology* 2006; **223**: 36–45.
25. Bartkova J, Horejsi Z, Koed K, Kramer A, Tort F, Zieger K *et al.* DNA-damage response as a candidate anti-cancer barrier in early human tumorigenesis. *Nature* 2005; **434**: 864–870.
26. Bourke E, Dodson H, Merdes A, Cuffe L, Zachos G, Walker M *et al.* DNA-damage induces Chk1-dependent centrosome amplification. *EMBO Rep* 2007; **8**: 603–609.
27. Hut HM, Lemstra W, Blaauw EH, Van Cappellen GW, Kampinga HH, Sibon OC. Centrosomes split in the presence of impaired DNA integrity during mitosis. *Mol Biol Cell* 2003; **14**: 1993–2004.
28. Lukasiewicz KB, Lingle WL, Aurora A. centrosome structure, and the centrosome cycle. *Environ Mol Mutagen* 2009; **50**: 602–619.
29. Kleylein-Sohn J, Westendorf J, Le Clech M, Habedanck R, Stierhof YD, Nigg EA. Plk4-induced centriole biogenesis in human cells. *Dev Cell* 2007; **13**: 190–202.
30. Bettencourt-Dias M, Glover DM. Centrosome biogenesis and function: centrosomics brings new understanding. *Nat Rev Mol Cell Biol* 2007; **8**: 451–463.
31. Duensing A, Liu Y, Perdreau SA, Kleylein-Sohn J, Nigg EA, Duensing S. Centriole overduplication through the concurrent formation of multiple daughter centrioles at single maternal templates. *Oncogene* 2007; **26**: 6280–6288.
32. Khodjakov A, Rieder CL, Sluder G, Cassels G, Sibon O, Wang CL. De novo formation of centrosomes in vertebrate cells arrested during S phase. *J Cell Biol* 2002; **158**: 1171–1181.
33. Tsou MF, Stearns T. Mechanism limiting centrosome duplication to once per cell-cycle. *Nature* 2006; **442**: 947–951.
34. Vogel C, Hager C, Bastians H. Mechanisms of mitotic cell death induced by chemotherapy-mediated G2 checkpoint abrogation. *Cancer Res* 2007; **67**: 339–345.
35. Ogden A, Padmashree CG, Aneja R. Let's huddle to prevent a muddle: centrosome declustering as an attractive anticancer strategy. *Cell Death Differ* 2012; e-pub ahead of print 1 June 2012; doi:10.1038/cdd.2012.61.
36. Xu FL, Saunders WS. Actin and microtubules: working together to control spindle polarity. *Cancer Cell* 2008; **14**: 197–199.
37. Castedo M, Perfettini JL, Roumier T, Andreau K, Medema R, Kroemer G. Cell death by mitotic catastrophe: a molecular definition. *Oncogene* 2004; **23**: 2825–2837.
38. Fukasawa K. P53, cyclin-dependent kinase and abnormal amplification of centrosomes. *Biochim Biophys Acta* 2008; **1786**: 15–23.
39. Weaver BA, Silk AD, Montagna C, Verdier-Pinard P, Cleveland DW. Aneuploidy acts both oncogenically and as a tumor suppressor. *Cancer Cell* 2007; **11**: 25–36.
40. Fukasawa K. Centrosome amplification, chromosome instability and cancer development. *Cancer Lett* 2005; **230**: 6–19.
41. Sluder G, Lewis K. Relationship between nuclear DNA synthesis and centrosome reproduction in sea urchin eggs. *J Exp Zool* 1987; **244**: 89–100.
42. Balczon R, Bao L, Zimmer WE, Brown K, Zinkowski RP, Brinkley BR. Dissociation of centrosome replication events from cycles of DNA synthesis and mitotic division in hydroxyurea-arrested Chinese hamster ovary cells. *J Cell Biol* 1995; **130**: 105–115.
43. Meraldi P, Nigg EA. The centrosome cycle. *FEBS Lett* 2002; **521**: 9–13.
44. Nigg EA, Raff JW. Centrioles, centrosomes, and cilia in health and disease. *Cell* 2009; **139**: 663–678.
45. Tibbetts RS, Brumbaugh KM, Williams JM, Sarkaria JN, Cliby WA, Shieh SY *et al.* A role for ATR in the DNA-damage-induced phosphorylation of p53. *Genes Dev* 1999; **13**: 152–157.
46. Shinozaki T, Nota A, Taya Y, Okamoto K. Functional role of Mdm2 phosphorylation by ATR in attenuation of p53 nuclear export. *Oncogene* 2003; **22**: 8870–8880.
47. Isaacs WB, Carter BS, Ewing CM. Wild-type p53 suppresses growth of human prostate cancer cells containing mutant p53 alleles. *Cancer Res* 1991; **51**: 4716–4720.
48. Sluder G, Khodjakov A. Centriole duplication: analogue control in a digital age. *Cell Biol Int* 2010; **34**: 1239–1245.
49. Loncarek J, Hergert P, Magidson V, Khodjakov A. Control of daughter centriole formation by the pericentriolar material. *Nat Cell Biol* 2008; **10**: 322–328.
50. Palazzo RE, Vaisberg E, Cole RW, Rieder CL. Centriole duplication in lysates of spisula solidissima oocytes. *Science* 1992; **256**: 219–221.
51. Szollosi D, Calarco P, Donahue RP. Absence of centrioles in the first and second meiotic spindles of mouse oocytes. *J Cell Sci* 1972; **11**: 521–541.
52. Calarco-Gillam PD, Siebert MC, Hubble R, Mitchison T, Kirschner M. Centrosome development in early mouse embryos as defined by an autoantibody against pericentriolar material. *Cell* 1983; **35**(3 Pt 2): 621–629.
53. Szollosi D, Ozil JP. De novo formation of centrioles in parthenogenetically activated, diploidized rabbit embryos. *Biol Cell* 1991; **72**: 61–66.
54. Marshall WF, Vucica Y, Rosenbaum JL. Kinetics and regulation of de novo centriole assembly. Implications for the mechanism of centriole duplication. *Curr Biol* 2001; **11**: 308–317.
55. Habedanck R, Stierhof YD, Wilkinson CJ, Nigg EA. The polo kinase Plk4 functions in centriole duplication. *Nat Cell Biol* 2005; **7**: 1140–1146.
56. Hinchcliffe EH, Miller FJ, Cham M, Khodjakov A, Sluder G. Requirement of a centrosomal activity for cell-cycle progression through G1 into S phase. *Science* 2001; **291**: 1547–1550.

Supplementary Information accompanies the paper on Cell Death and Disease website (http://www.nature.com/cddis)